Confined thin films of linear and branched alkanes

Marjolein Dijkstra[a)]
Shell Research and Technology Centre Amsterdam, Badhuisweg 3, 1031 CM Amsterdam, The Netherlands

(Received 21 January 1997; accepted 13 May 1997)

We report computer simulations in the Grand canonical ensemble of a system of several alkanes between two solid surfaces. We computed the solvation force exerted by the fluid on the plates. The solvation force for linear decane oscillates with distance with a periodicity close to the width of the molecules. The branched alkanes (2-methylundecane and 2-methylheptane) show a similar oscillatory behavior, however the oscillations are decreased and are shifted to the attractive regime. In addition, we computed the liquid-vapour equilibria by using Gibbs ensemble Monte-Carlo simulations of *n*-pentane confined in a slit of 9, 13, 17 Å. The critical temperature of the liquid-vapour coexistence shifts to lower temperatures upon confining. At a plate separation of 5 Å, no liquid-vapour equilibrium is found. © *1997 American Institute of Physics.*
[S0021-9606(97)51131-7]

I. INTRODUCTION

The behavior of fluids in contact with solid surfaces or confined in microscopic pores is of fundamental as well as practical importance. They play an important role in applications as engine lubrication, zeolites, clay swell or in the stability of colloidal systems, like emulsions, paints, surface coatings, etc. The molecular structure of the confined fluid can differ dramatically from that in the bulk. It is therefore that we cannot use our knowledge of bulk fluids, when we are dealing with fluids in confined geometries. Due to the technological importance significant experimental and theoretical effort has been dedicated to this subject. The background of fluids adsorbed in narrow pores is described in a review article by Evans.[1]

Historically, the DLVO theory (Derjaguin-Landau-Verwey-Overbeek) and the Van der Waals theory have been used to describe colloidal stability in bulk systems.[2,3] However, if two particles or surfaces approach each other closer than a few molecular diameters, these theories have been found to be inadequate to predict the interactions between the surfaces, since other forces become important.[4] These short-range forces are called solvation forces, or hydration forces in the case of water.

Experimentally, the surface force apparatus can be used to measure very accurately the forces acting on two solid surfaces immersed in a fluid.[4,5] These short-range solvation forces were found to be monotonically repulsive, monotonically attractive or oscillatory with distance. The oscillatory behavior of the solvation force is now well-understood for simple spherical molecules. Theoretical work and computer simulations of Lennard-Jones fluids and hard spheres show that the oscillatory solvation force originates from the ordering of the molecules in layers when the fluid is confined by the surfaces.[6–19] For finite ranged wall-fluid and fluid-fluid potentials, the solvation force shows an oscillatory behavior at high liquid densities and a pure exponential decay at low liquid densities, provided the liquid is sufficiently far from the critical point and no phase transition will occur.

Besides, the structure of the solvation force, oscillatory or monotonically decaying, depend strongly on the chemical and physical nature of the surfaces, for example, whether they are hydrophilic, hydrophobic, smooth, corrugated etc. On the other hand, the oscillatory behavior is very sensitive for the detailed chemical structure of the molecules and the ability of the molecules to order. One of the most striking examples of this sensitivity is the difference between the solvation force of linear and branched alkanes. For example, experiments showed that a single methyl side group on a linear octadecane chain can completely eliminate the oscillations in the solvation force.[20,21] This phenomenon may be the reason why branched alkanes are better lubricants than linear ones. A similar difference was observed in force measurements of low molecular weight polymer melts. Unbranched polydimethylsiloxane (PDMS) exhibits a short-range oscillatory solvation force profile, while branched polybutadiene (PB) shows only a monotonically repulsive solvation force.[22,23] However, recent computer simulations of octane and isooctane did not reveal this unexpected difference in the solvation force profiles, casting doubts on the experiments.[24] Also recent experiments of 3-methylundecane show that the solvation force shows still an oscillatory behavior, however the amplitudes of the oscillations are smaller than for linear undecane.[25] In this article, we show by computer simulations that there is a difference in the solvation force for branched and unbranched alkanes. Our results show an oscillatory behavior for the solvation force of linear decane with a periodicity close to the width of the alkanes. For 2-methylundecane and 2-methylheptane, we still found oscillations in the solvation force, but the amplitudes of the oscillations are decreased with respect to *n*-decane. The solvation force, however, is shifted to the attractive region. A preliminary account of parts of this work has been published elsewhere.[26]

In order to investigate if our state points were sufficiently far from the critical point, we located the liquid-

a)Present address: H.H. Wills Physics Laboratory, Royal Fort, Tyndall Avenue, Bristol BS8 1TL, United Kingdom.

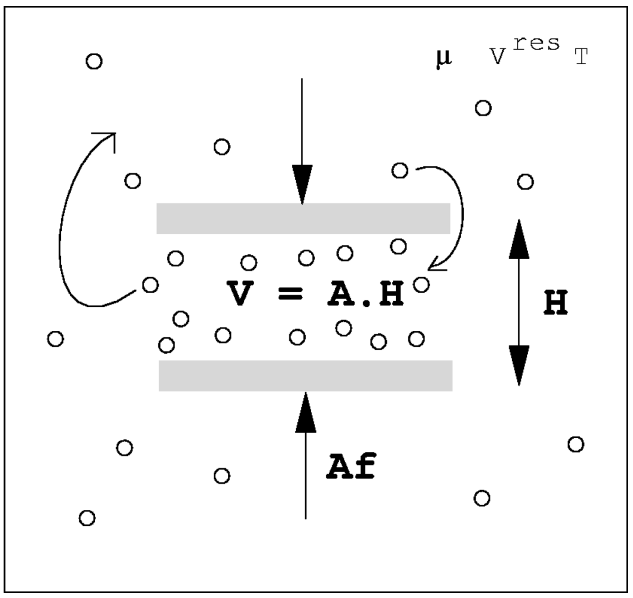

FIG. 1. Schematic picture of a surface force apparatus.

vapour transition for the confined fluid. In its own right it is already an interesting question what will happen to the liquid-vapour transition upon confining. Will it still exist or will it shift with respect to the bulk liquid-vapour transition? In section V, we will show that the critical temperature of the liquid-vapour coexistence shifts to lower temperatures upon confining and that the density of the liquid in the simulations for the solvation force were sufficiently far from the critical point.

II. MONTE-CARLO CALCULATIONS

The surface force apparatus measures the force between two molecularly smooth mica surfaces immersed in a fluid as a function of the distance. The confined fluid between the surfaces is, thus, in equilibrium with the bulk fluid outside the plates. This apparatus can, hence, be considered as a system of volume $V^{\rm res}$ with two plates with an area A held at a distance H apart in a fluid with a chemical potential μ. A schematic picture of the system is shown in Fig. 1. At small plate separation, the structure of the confined fluid differs substantially from that of the bulk, and hence a net force is exerted perpendicular to the plates. This solvation force can be measured by the surface force apparatus.

Below, we will describe the thermodynamics of this system in order to derive an expression of the solvation force. We refer the reader to Ref. 27 for more details. When we describe the thermodynamics of such an open system, we should consider the grand potential $\Omega=U-TS-\mu N$, where U is the internal energy, S the entropy, T the temperature, and N the number of particles. The change in the grand potential of this system is[27]

$$d\Omega=-p^b dV^{\rm res}-SdT-Nd\mu+2\gamma dA-Afd H, \tag{1}$$

where p^b is the bulk pressure, $V^{\rm res}$ is the volume of the whole reservoir, and f the solvation force. The plate-fluid interfacial tension γ is given by:

$$\gamma=\frac{1}{2}\left(\frac{\partial\Omega}{\partial A}\right)_{V,T,\mu,H}. \tag{2}$$

The last two contributions are due to the confinement. We now consider the same reservoir with the same volume and chemical potential but without the plates:

$$d\Omega=-p^b dV^{\rm res}-S^b dT-N^b d\mu. \tag{3}$$

If we now define the surface excess functions

$$\Omega^{\rm ex}=\Omega-\Omega^b,$$

$$S^{\rm ex}=S-S^b=2As,$$

$$N^{\rm ex}=N-N^b=A\Gamma,$$

we obtain

$$d\Omega^{\rm ex}=-2AsdT-A\Gamma d\mu+2\gamma dA-Afd H. \tag{4}$$

The surface excess functions separate the surface terms from the bulk terms. For a bulk system, the grand potential $\Omega^b(\mu,V,T)$ is equal to:

$$\Omega^b(\mu,V,T)=-p^b(\mu,T)V \tag{5}$$

as the volume of the system is an extensive quantity. For a confined system, there is an additional contribution to the grand potential due to the surfaces, which is extensive in the area of a single wall A,

$$\Omega(\mu,V,A,H,T)=-p^b(\mu,T)V+2\gamma(\mu,H,T)A. \tag{6}$$

If we now consider a confined volume $V=AH$, the grand potential of the whole system can be written as:

$$\Omega(\mu,A,H,T)=A[-p^b(\mu,T)H+2\gamma(\mu,H,T)] \tag{7}$$

such that in a semi-infinite system ($H\to\infty$), the grand potential contains only a bulk contribution, i.e.,

$$\lim_{H\to\infty}\Omega=-p^bAH \tag{8}$$

leading to the following condition:

$$\lim_{H\to\infty}2\gamma/H=0. \tag{9}$$

This condition is satisfied as in the limit $H\to\infty, 2\gamma\to\gamma_1+\gamma_2$ is constant, where γ_1 and γ_2 are the

interfacial tensions for the fluid with plate 1 and 2, respectively. If we now consider the surface excess functions $\Omega^{ex}=2\gamma A$, the differential of Ω^{ex} is:

$$d\Omega^{ex}=2\gamma dA+2Ad\gamma \tag{10}$$

$$=2\gamma dA+2A\left[\left(\frac{\partial\gamma}{\partial\mu}\right)_{T,H}d\mu+\left(\frac{\partial\gamma}{\partial T}\right)_{\mu,H}dT+\left(\frac{\partial\gamma}{\partial H}\right)_{\mu,T}dH\right]. \tag{11}$$

This expression should be equal to Eq. 4, which leads to the following relations:

$$\Gamma=-2\left(\frac{\partial\gamma}{\partial\mu}\right)_{T,H}, \tag{12}$$

$$s=-\left(\frac{\partial\gamma}{\partial T}\right)_{\mu,H}, \tag{13}$$

$$f=-2\left(\frac{\partial\gamma}{\partial H}\right)_{\mu,T}. \tag{14}$$

In the limit $H\rightarrow\infty$, the interfacial tension $2\gamma\rightarrow$ constant, and hence, we find that $f\rightarrow 0$ for a semi-infinite system.

Using that $\Omega^{ex}=2\gamma A$ and $\Omega^{b}=-p^{b}V=-p^{b}AH$, we obtain

$$\gamma=\frac{1}{2A}[\Omega+p^{b}AH] \tag{15}$$

and the solvation force reads

$$f=-\frac{1}{A}\left(\frac{\partial\Omega}{\partial H}\right)_{\mu,T,A}-p^{b}=p^{*}-p^{b}. \tag{16}$$

For a system with a plate at $z=0$ and $z=H$, the fluid-wall potential can be written as $V_{ext}(z)=V_{s}(z)+V_{s}(H-z)$. The pressure p^{*} can now be computed as follows:[28]

$$p^{*}=-\frac{1}{A}\left(\frac{\partial\Omega}{\partial H}\right)_{\mu,T,A}=-\int_{0}^{H}dz\rho(z)\frac{\partial V_{ext}(z)}{\partial H}. \tag{17}$$

By symmetry, we find that the force on the upper surface is equal to the force on the lower surface:

$$p^{*}=\int_{0}^{H}dz\rho(z)\frac{\partial V_{s}(H-z)}{\partial z}=-\int_{0}^{H}dz\rho(z)\frac{\partial V_{s}(z)}{\partial z}. \tag{18}$$

In order to compute the solvation force correctly in a simulation, we have to perform simulations for different plate separations at a fixed chemical potential while the number of particles fluctuates. We therefore performed Grand canonical Monte Carlo (GCMC) simulations of alkanes between two plates, where the independent variables are the chemical potential μ, the volume $V=AH$ and the temperature T. In order to obtain a fixed chemical potential, particles are exchanged with a fictitious infinitely large reservoir which contains an ideal gas of the same particles (in the present case the particles in the reservoir have internal energies).[29]

TABLE I. Details of the potential model used in this work for linear alkane (Ref. 30).

Linear alkanes	
Nonbonded	$\epsilon_{CH_3}=114.0$ K $\epsilon_{CH_2}=47.0$ K $\sigma_{CH_3}=3.93$ Å $\sigma_{CH_2}=3.93$ Å truncated at 13.8 Å
Bond length	$l_B=1.54$ Å
Bond bending	$k_\theta=62\,500$ K rad^{-2} $\theta_0=114°$
Torsion	$c_0=0$ $c_1=355.03$ K $c_2=-68.19$ K $c_3=791.32$ K

The alkanes are modeled by the united atom approximation, where every CH_3 or CH_2 group is described as a single interaction site. The non-bonded dispersive interactions between these ''united atoms'' of different molecules or within a molecule (when two atoms are more than four atoms apart) are described with a Lennard-Jones potential:

$$u^{LJ}(r_{ij})=4\epsilon_{ij}\left[\left(\frac{\sigma_{ij}}{r_{ij}}\right)^{12}-\left(\frac{\sigma_{ij}}{r_{ij}}\right)^{6}\right]. \tag{19}$$

The potential parameters of unlike bead interactions are calculated using the Lorentz-Berthelot rules,

$$\epsilon_{ij}=\sqrt{\epsilon_i\epsilon_j},\quad \sigma_{ij}=\sqrt{\sigma_i\sigma_j}. \tag{20}$$

We used fixed bond lengths and a harmonic bond angle bending:

$$u^{bend}(\theta)=\tfrac{1}{2}k_\theta(\theta-\theta_0)^2. \tag{21}$$

Changes in the dihedral angle are described by a torsion potential:

$$u^{tors}(\phi)=c_0+0.5c_1(1+\cos\phi)+0.5c_2(1-\cos 2\phi)+0.5c_3(1+\cos 3\phi). \tag{22}$$

The parameters for the potentials of the linear alkanes were derived from calculations of the vapour-liquid phase equilibria of n-alkanes by Smit *et al.*[30] For the branched alkanes, we used the model of Wang *et al.*, which is based on Jorgensen's optimized potentials for liquid simulations (OPLS).[24] The parameters are listed in Tables I and II.

In our model, we confined the alkane fluid in the z-direction by two flat surfaces. However, experimentally, the force is measured between curved surfaces in the surface force apparatus, but using the Derjaguin approximation the force between curved surfaces can be related to an energy per unit area between flat surfaces.[4] In the vicinity of the surfaces, the alkanes experience a potential field due to the solid surfaces. In our simulations, we used a 9-3 wall-potential, which corresponds to the summation of the mean field atom-solid 10-4 potentials from different lattice planes of a solid consisting of Lennard-Jones particles,[31]

$$V_s(z)=\frac{2\pi\rho_s\epsilon_w}{3}\left(\frac{2\sigma_w^{12}}{15z^9}-\frac{\sigma_w^6}{z^3}\right). \tag{23}$$

Here we defined $\sigma_w=(\sigma_s+\sigma_i)/2$ with σ_s the size of the atoms of the solid surface. In our simulations we used $\sigma_s=2.22$ Å, which corresponds to the diameter of a typical metal atom and σ_i denotes the diameter of atom i. $\rho_s=\sqrt{2}/a_1^3$ is the density of atoms in the solid where the lattice parameter $a_1=1.098\sigma_s$. The depth of the attractive well of the atom-wall potential is determined by ϵ_w. The values of the parameters are taken from Ref. 32, where a simple 9-3 site-wall potential is introduced for a surface with some texture. However, in our calculations we ignore the corrugation of the surfaces (Table III).

Conventional Monte Carlo schemes are not sufficiently efficient to ensure rapid equilibration, as direct insertion of a flexible particle in a dense fluid almost always results in an overlap with one of the other chains in the fluid. For a faster equilibration of the alkanes, it is essential to use the configurational bias Monte-Carlo (CBMC) method.[33] In the CBMC-method, the construction of the alkane conformations proceeds atom by atom. To add an atom to the chain, we generate a fixed number of trial atoms in such a way that the probability of finding a given trial atom is given by the Boltzmann weight corresponding to the internal energy, i.e., the sum of the bond-bending potential and the torsion potential. We then choose one of the trial segments with a probability proportional to the external energy, i.e., the non-bonded interactions. This algorithm biases the insertion of chains in such a way that chains with favorable internal energies are inserted in regions with favorable external energies. Overlap with other chains is in this way avoided. For more technical details on the implementation of the CBMC-method, we refer the reader to Refs. 33, 30. When we regrow a part of the polymer, we cut the polymer at a random position, we remove one part of the polymer or the other and regrow that part. The branched alkanes (2-methylheptane and 2-methylundecane) have two indistinguishable end methyl groups at the second carbon atom. The construction of the branched chain ends always with the addition of the two indistinguishable end methyl groups. We found that it was essential to generate a set of two trial end methyl groups simultaneously in such a way that the probability of finding a given trial atom is given by the Boltzmann weight corresponding to the internal energies. We then choose one of the sets of trial atoms for the end methyl groups with a probability proportional to the external energies of both trial atoms.

Most runs consisted of at least 10^8 cycles. In each cycle, an attempt is made to regrow a part of the polymer using the CBMC-method and a removal or insertion of a particle in the box is attempted. On average, once every two cycles, a random displacement and random rotation of a particle in the box is attempted and once every five cycles, a whole polymer is regrown at a random place in the box using the CBMC-method.

TABLE II. Details of the potential model used in this work for branched alkane (Ref. 24).

Branched alkanes	
Nonbonded	$\epsilon_{CH_3}=88.06$ K
	ϵ_{CH_3} (branched end) $=80.51$ K
	$\epsilon_{CH_2}=59.38$ K
	$\epsilon_{CH}=40.25$ K
	$\sigma_{CH_3}=3.905$ Å
	σ_{CH_3} (branched end) $=3.910$ Å
	$\sigma_{CH_2}=3.905$ Å
	$\sigma_{CH}=3.850$ Å
	truncated at 9.626 Å
Bond length	$l_B=1.53$ Å
Bond bending	$k_\theta=63437$ K rad^{-2}
	$\theta_0=112.4°$
Torsion	$c_0=1460.44$ K
	$c_1=-384.147$ K
	$c_2=-134.174$ K
	$c_3=-434.619$ K

TABLE III. Details of the potential model used for the interaction between the atoms and the substrate (Ref. 32).

Substrate	
Site-wall potential	$\sigma_s=2.22$ Å
	$a_1=1.098\ \sigma_s$
	$\rho_s=\sqrt{2}/a_1^3$
	$\sigma_w=\frac{1}{2}(\sigma_s+\sigma_i)$
	$\epsilon_w/k=100.0$ K

III. RESULTS

GCMC simulations were performed on a system of decane, 2-methylheptane and 2-methylundecane. The fluid is confined in z-direction by solid surfaces of 34 Å × 34 Å. The plate separations vary from 5–50 Å. In the x- and y-direction, we used periodic boundary conditions, such that an infinite, periodic system is simulated. In all the simulations the temperature T is fixed at a value of 298 K and the chemical potential is such that the density of the reservoir is 0.717 ± 0.008 g/cm^3 for all species, which corresponds to a liquid phase. In our simulations, we measured the solvation

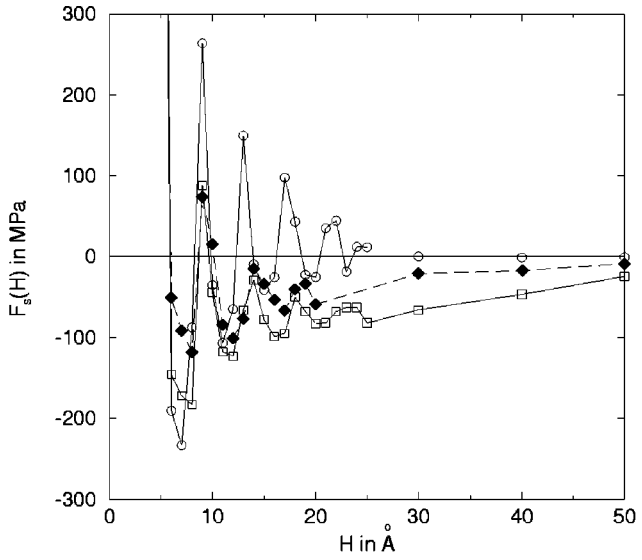

FIG. 2. The solvation force in MPa versus the distance H of the plates in Å for *n*-decane (open circles), 2-methylheptane (filled diamonds), and 2-methylundecane (open squares).

force p^* by averaging the solvation force on the upper and lower plate (Eq. 18):

$$p^* = \left\langle -\frac{1}{2A}\left[\sum_{i=1}^{N}\frac{\partial V_s(z_i)}{\partial z_i} - \frac{\partial V_s(H-z_i)}{\partial z_i}\right]\right\rangle, \tag{24}$$

where $V_s(z)$ is the 9-3 site-wall potential, N the number of particles and the brackets $\langle\cdots\rangle$ denote the ensemble average $\langle\cdots\rangle_{\mu,T,H}$. Note that we did not subtract the bulk pressure in this equation. The bulk pressure was found to be small compared to the solvation force.

In Fig. 2, we plot the solvation force versus the distance H between the plates for *n*-decane, 2-methylheptane and 2-methylundecane. For *n*-decane, we observe strong oscillations with a periodicity of 4–4.5 Å. However, in the case of 2-methylheptane and 2-methylundecane, the oscillations are less pronounced and are shifted to the attractive region. At large plate separations, the solvation force for the branched alkanes goes to zero as it should be from a thermodynamic point of view. For 2-methylheptane the solvation force becomes zero at plate separations larger than 30 Å. For 2-methylundecane, we find that the solvation force goes to zero very slowly with increasing plate separation. In Fig. 3, we plot the density distribution $\rho(z)$ of decane at different values for the plate separation. No adsorption of alkanes are found for distances smaller than 5 Å. We observe one fluid layer for a plate distance of 5 Å. For a separation of 6–12 Å, two layers are formed. Three layers are observed for a separation of 13–16 Å, four layers for distances of 17–21 Å, and five layers for distances of 22–26 Å. If we compare these density distributions with the solvation force, we observe clearly that one sharp peak at a distance of 5 Å corresponds with a high value for the solvation force. When we increase the distance we find that two layers are formed, but they do not fit perfectly between the surfaces: the solvation force drops, i.e., the fluid can be squeezed out easily. At a distance of 9 Å, we observe two sharp peaks corresponding with a high solvation force. By increasing the distance further the peaks become broader and the solvation force drops. At a distance of 13 Å, three well-defined layers are formed: the solvation force is high. The solvation force decreases with increasing distance until at a distance of 17 Å, a fourth layer appears. Again the two layers in the middle do not fit well and the solvation force increases when we increase the distance. At a distance of 18 Å, four sharp peaks are observed, etc. We can conclude that the origin of the oscillations in the solvation force lies in the ordering of the chains in layers. When the density distributions show sharp peaks, i.e., when the fluid orders in well-defined layers, the solvation force is high, i.e., it is difficult to squeeze out the fluid between the plates. The solvation force drops when the density distributions are broader, i.e., when it is difficult for the molecules to form well-defined layers. In Fig. 4, we plot the density profiles of 2-methylundecane and that of the end methyl groups at the branching site for varying plate separations. We observe that the profiles of decane are more strongly peaked than those of 2-methylundecane. We also observe from the density profiles for the branched methyl groups that one branched methyl group is in the fluid layer, while the other lies between the fluid layers. As the solvation force depends on the formation of well-defined layers between the plates, we plot for comparison in Fig. 5 the density profile of *n*-decane and 2-methylundecane in the same figure, when one, two, three and four well-defined layers are formed between the plates. We took the density profiles at the maxima of the oscillations. We observe that the density profiles for *n*-decane are more strongly peaked that those of 2-methylundecane.

In Fig. 6, we plotted the density in g/cm^3 of the confined fluids as a function of plate separation. The volume of the slab is estimated as the space that is available for the alkanes, i.e., $V=A\times(H-2\delta)$, where δ is the minimum distance at which a methylene subunit can approach the wall. We estimated the value of δ to be about 0.6 Å. We found that the density for *n*-decane oscillates with plate separation around the bulk density. The densities of 2-methylundecane and 2-methylheptane are on average lower than the one for *n*-decane. We observe that the density of 2-methylheptane is lower than for 2-methylundecane. This might be explained by the difference in the ratio of CH_3 and CH_2-groups in 2-methylheptane and 2-methylundecane. Surprisingly, the solvation force for 2-methylundecane is more attractive than the one for 2-methylheptane, while $\rho(H)$ for 2-methylundecane is closer to the one of *n*-decane. One reason for this might be that the ability of the molecules to form well-defined layers is larger for 2-methylheptane than for 2-methylundecane, as the chains are shorter.

In Fig. 7, we show a typical configuration of a layer of *n*-decane at $H = 5$ Å. The density of this film is close to the bulk liquid density of *n*-decane and the alkanes are disor-

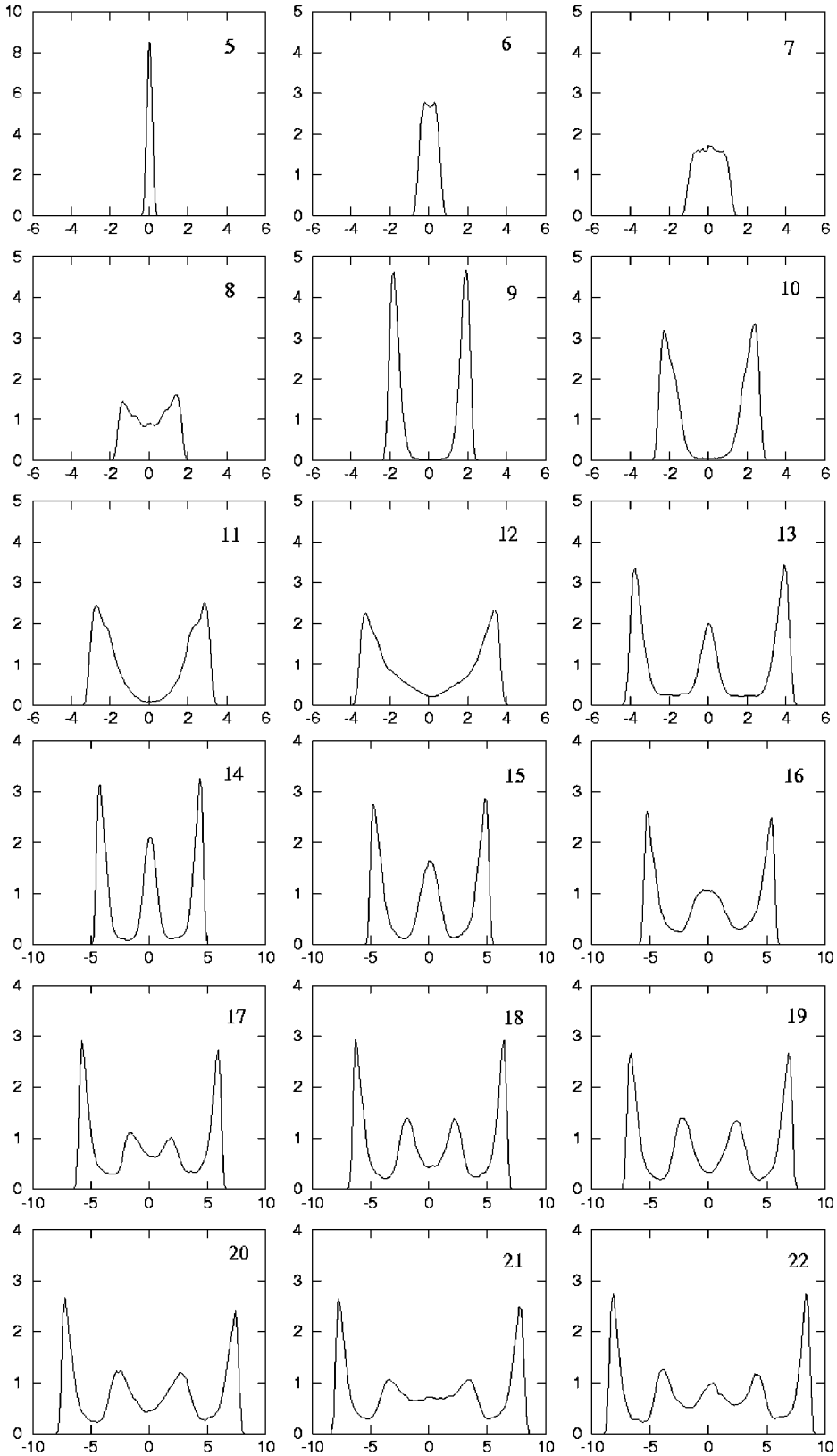

FIG. 3. Density distribution $\rho(z)$ in g/cm^3 of n-decane at different values for the plate separation. The plate separation in Å is written in the figures.

dered in position and orientation. We therefore conclude that the configuration is fluid-like. In Figs. 8, 9, and 10 typical snapshots are shown of n-decanes and 2-methylundecanes adsorbed in a slit with a slitwidth of 9 Å, 13 Å(n-decane) and 14 Å(2-methylundecane), and 17 Å(n-decane) and 18 Å(2-methylundecane), respectively. We clearly see that discrete fluid layers are formed in the case of n-decanes, while the fluid is more homogeneous in the case of 2-methylundecane.

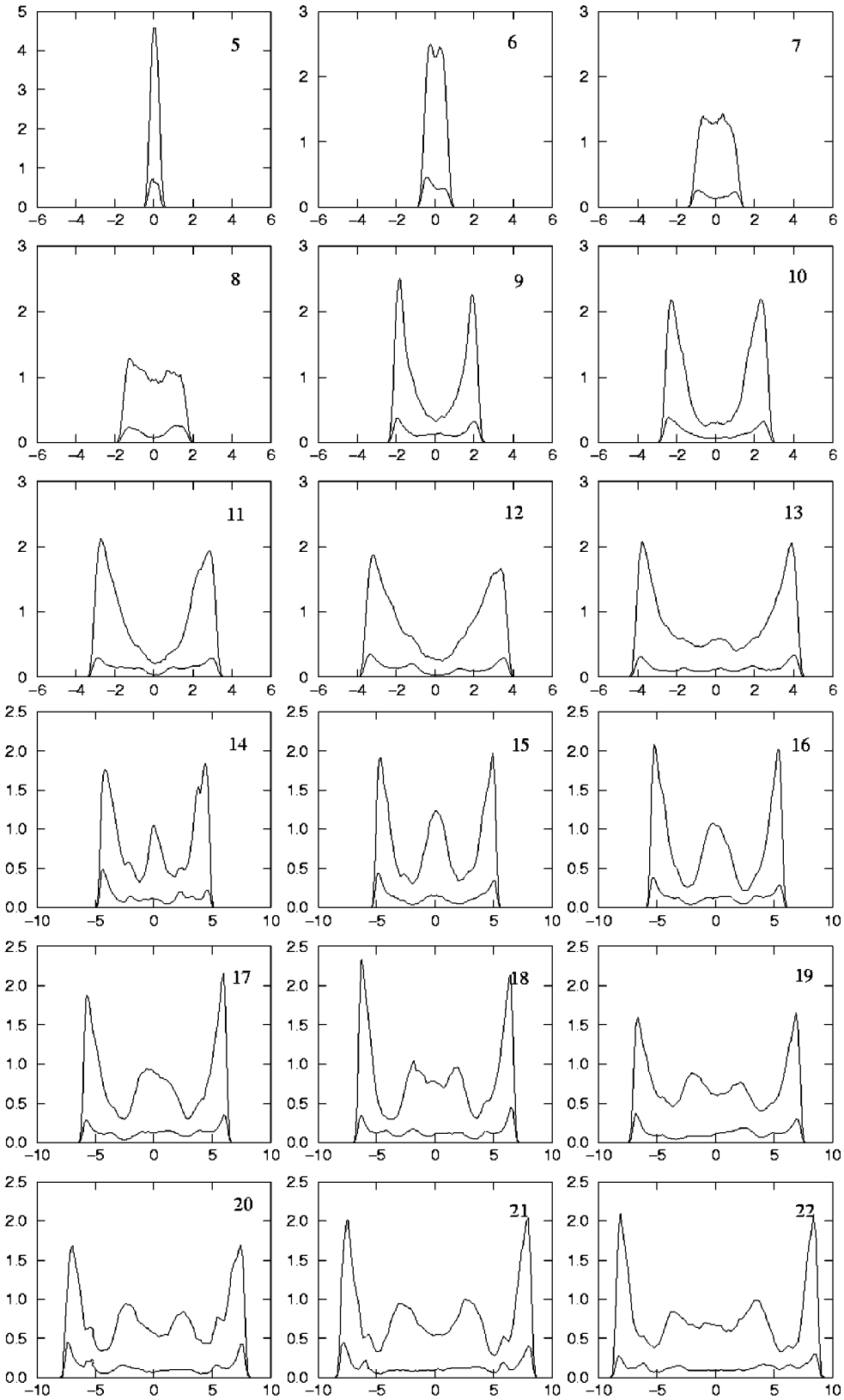

FIG. 4. Density distribution $\rho(z)$ in g/cm^3 of 2-methylundecane (upper solid line) and that of the end methyl groups (lower solid line) at different values for the plate separation. The plate separation in Å is written in the figures.

In order to investigate in more detail the structure of the fluid, we compute the orientational distribution functions as a function of z. For alkane molecules, that can be in the cis or $trans$ state, it is convenient to consider two angles θ_l and θ_p. For each set of three successive atoms, θ_l is defined as the angle between the vector between the two end atoms in the set with the normal of the walls and θ_p is defined as the angle between the normal of the plane of the three atoms

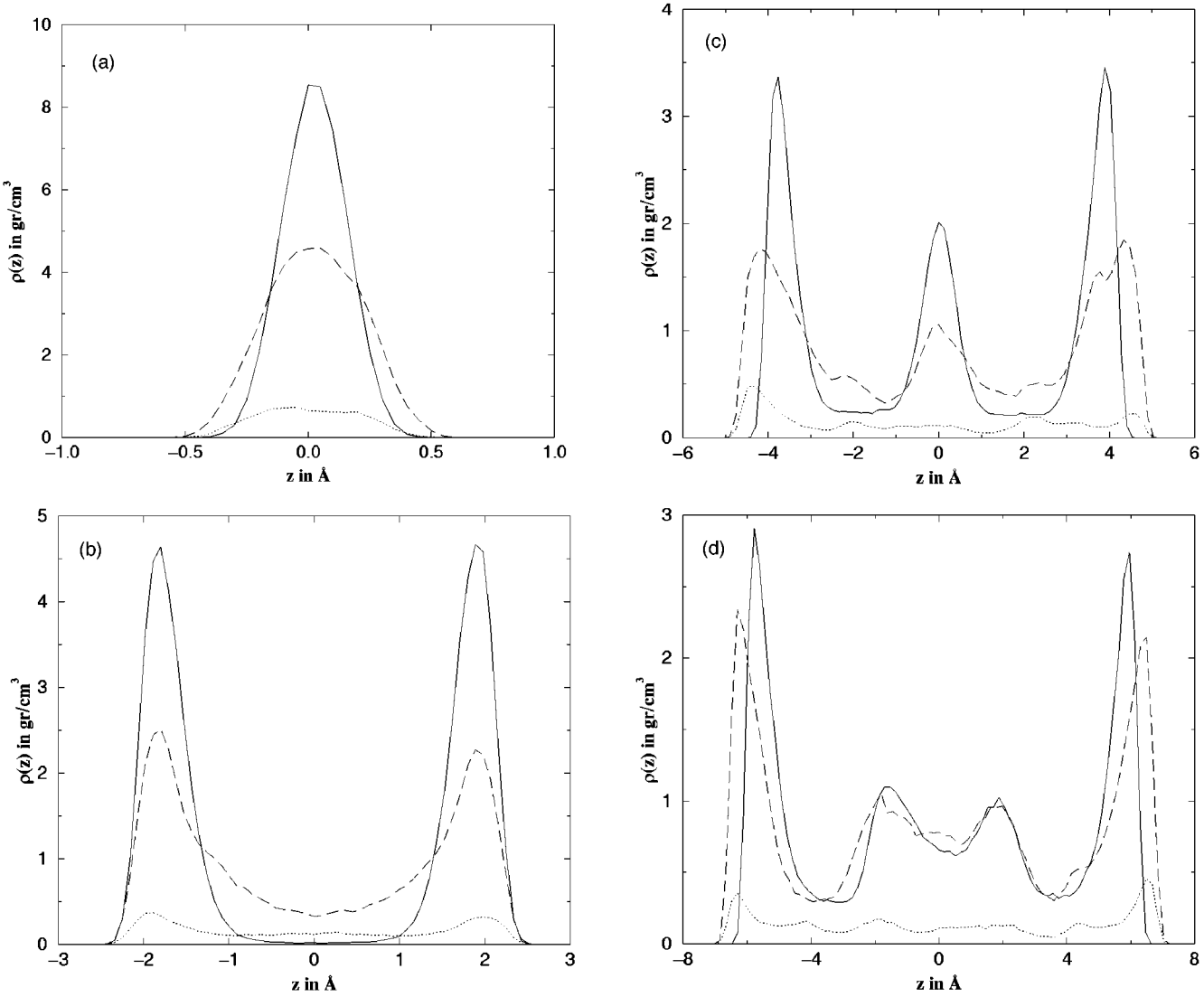

FIG. 5. Density distribution $\rho(z)$ in g/cm^3 of n-decane (solid line) and 2-methylundecane (dashed line) and that of the end methyl groups of 2-methylundecane (dotted line) versus z in Å for a plate separation of (a) 5 Å, (b) 9 Å, (c) 13 Å for n-decane and 14 Å for 2-methylundecane, and (d) 17 Å for n-decane and 18 Å for 2-methylundecane.

with the normal of the walls.[24] The orientational distribution functions $P_l(z)$ and $P_p(z)$ are now defined as:

$$P_{l,p}(z)=\tfrac{1}{2}\langle 3\cos^2\theta_{l,p}(z)-1\rangle. \tag{25}$$

If all the molecules are parallel to the walls and in the all-*trans* state, $P_l(z)$ is $-1/2$ and if the chains are perpendicular to the wall $P_l(z)$ is 1.0. As all the planes of three successive molecules in the chain are parallel to the wall, $P_p(z)$ is 1.0. The order parameters are zero when the chains are randomly oriented. In Fig. 11, we plot $P_l(z)$ and $P_p(z)$ for a plate separation of 5 Å for n-decane and 2-methylundecane. For both species, $P_l(z)$ is $-1/2$ for all z, which means that all the molecules are parallel to the walls. However, $P_p(z)$ depends on z: close to the walls the order parameter is lower than in the middle of the slit. For 2-methylundecane, it even drops to -0.2, which denotes that the planes in the chains are randomly oriented. In Figs. 12 and 13, we plot $P_l(z)$ and $P_p(z)$ for a plate separation of 9 and 13 Å for n-decane and 2-methylundecane. We observe that the chains are ordered within the fluid layers ($P_l(z)$ is about -0.45 and -0.4 for n-decane and 2-methylundecane and $P_p(z)$ is positive for both species), but are randomly oriented between the layers ($P_l(z)$ and $P_p(z)$ go to zero).

IV. DISCUSSION

If we compare our results with the experimental data of Refs. 20, 25, we observe two remarkable features. First of all, we still find oscillations in the solvation force of branched alkanes. From Figs. 2, 3, 4, 5, 8, 9, and 10 we can conclude that the origin of oscillations in the solvation force lies in the ordering of the molecules in fluid layers. In the case of n-decane, well-defined fluid layers are formed. However, the ability of branched alkanes to form discrete layers is reduced due to simple packing arguments, but is not com-

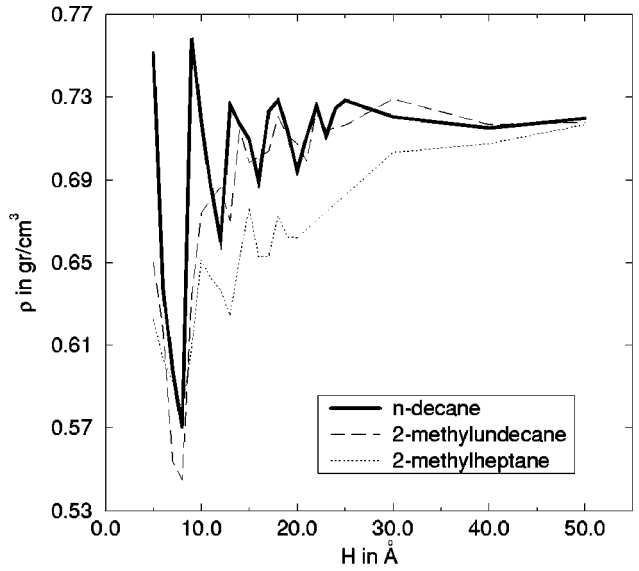

FIG. 6. The density in g/cm^3 of between the plate of n-decane, 2-methylheptane, and 2-methylundecane versus the plate separation.

pletely eliminated, as can be seen in Figs. 4, 5, 8, 9, and 10. This explains the two or three times weaker oscillations in our results in the case of branched alkanes, which agrees well with Granick's experiments of 3-methylundecane and linear undecane. In the experiments of Israelachvili *et al.*, no oscillations are found in the solvation force. However, their results show that the solvation force could not be measured accurately and a degree of scatter is found in their data of the same order of the amplitudes of the oscillations in Granick's data. The other surprising feature in our results is that the solvation force of branched alkanes is shifted to the attractive region. From the density profiles of Fig. 5, we can understand why the branched alkanes exhibit a predominantly attractive force between the plates. The reason is that repulsive

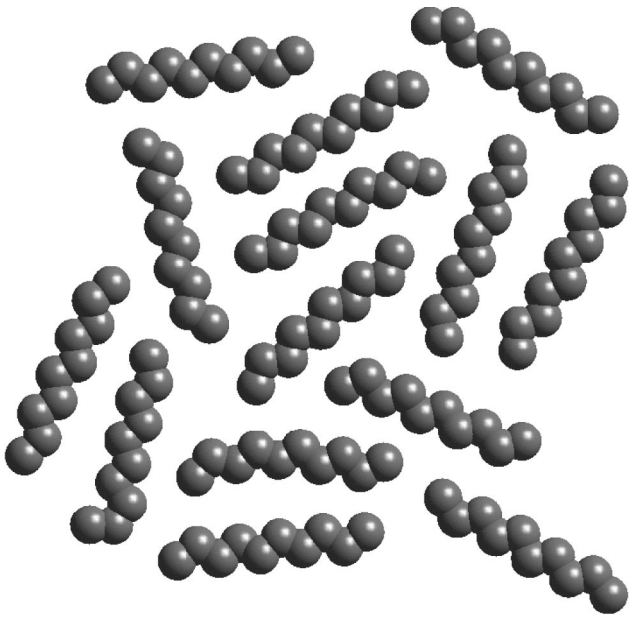

FIG. 7. Typical snapshot of n-decane (xy-plane) at a plate separation of 5 Å.

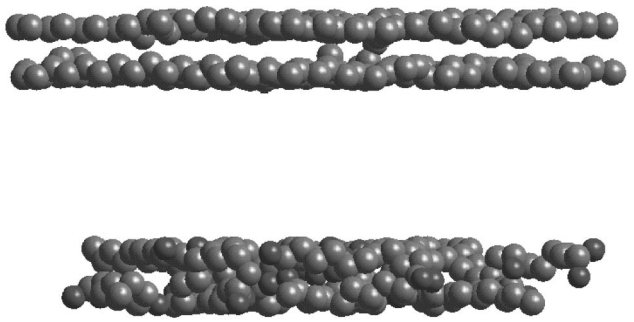

FIG. 8. Typical snapshots of n-decane (top) and 2-methylundecane (bottom) at a plate separation of 9 Å.

contributions to the solvation force stem only from particles close to the wall, i.e., $-\partial V_s(z)/\partial z>0$ when $z<2.6395$ Å. Thus, a repulsive solvation force can only be obtained when there is a strong ordering of molecules close to the wall. Fig. 5 shows that in the case of branched alkanes, the ordering of the molecules close to the wall is smaller in comparison with n-decanes. This is the reason why an attractive solvation force is obtained for branched alkanes. This attractive solvation force agrees with the experiments of Israelachvili *et al.* They observed a long-range attractive force at least until a plate separation of 30 Å. In the surface force experiments force differences are measured by changing the plate separation with respect to the force at a certain plate separation. Thus the solvation force measured in the experiments depends strongly on the plate separation at which the zero level of the force is taken. On the other hand, the force measurements are sensitive to the stiffness of the force measuring spring and on the equilibration time used for each force measurement. These factors may explain why Granick *et al.* found oscillations in the solvation force around zero, while Israelachvili *et al.* only found a long-range attractive force in their experiments.

A reason for the long-range attractive force may be as follows. The branched methyl groups frustrate the packing of the molecules in one layer and the molecules will have the tendency to leave the layer. The amount of interdigitation, i.e., in what extent individual molecules go from one layer to another, will increase. In Ref. 34, it is already shown that

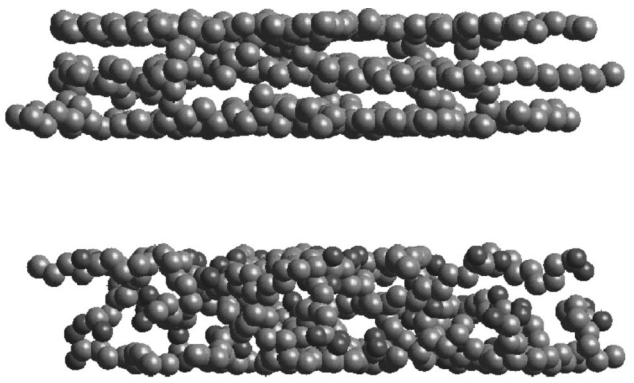

FIG. 9. Typical snapshots of n-decane (top) and 2-methylundecane (bottom) at a plate separation of 13 Å for n-decane and 14 Å for 2-methylundecane.

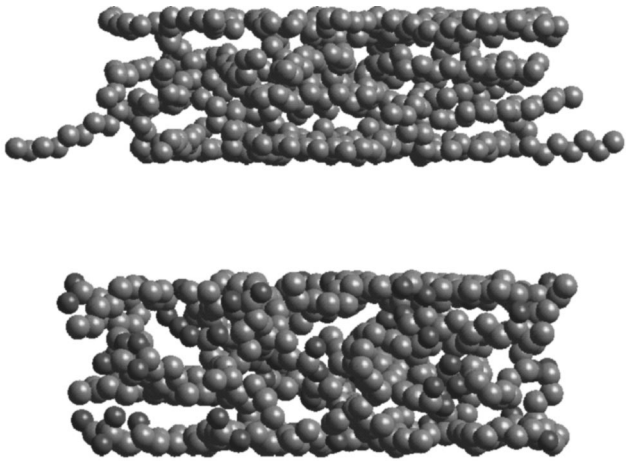

FIG. 10. Typical snapshots of *n*-decane (top) and 2-methylundecane (bottom) at a plate separation of 17 Å for *n*-decane and 18 Å for 2-methylundecane.

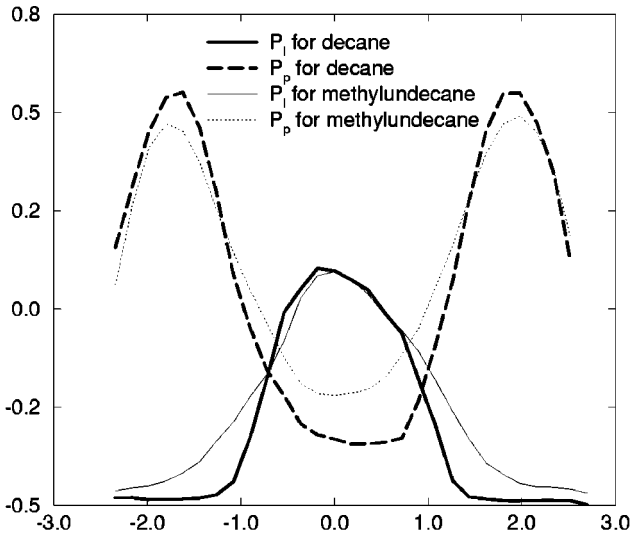

FIG. 12. The order parameters $P_l(z)$ and $P_p(z)$ for a plate separation of 9 Å for *n*-decane and 2-methylundecane.

molecules with many side branches (like squalane) reveal a large amount of interdigitation near a single wall. These links between the individual layers may be the reason for this long-range attractive force. The solvation force for 2-methylundecane is more attractive than the solvation force for 2-methylheptane. This might be explained by the fact that 2-methylheptane has a higher ability to order themselves in well-defined layers, as the chains are shorter.

In the simulations of Wang *et al.* no remarkable difference is found in the solvation force between linear octane and branched iso-octane. However, if we compare the results of the solvation force in more detail, we find that the maxima in our solvation force have a value of 266, 153, and 99 MPa (Fig. 2), in comparison with much lower values (86.5, 32.6 and 13.7 MPa) in their results. This is caused by a much higher density of alkanes between the plates in our simulations. In the simulations of Wang *et al.* the molecules could flow in and out the slab and could evaporate and condensate in order to mimic a liquid droplet in a slit that is in equilibrium with its vapour. The resulting alkane density is, hence, 0.55–0.60 g/cm^3 in the slit, which is in the metastable region of the liquid-vapour coexistence.

V. PORE CONDENSATION

In order to investigate if the state points for measuring the solvation force were sufficiently far from the critical point, we located the liquid-vapour coexistence region for the confined fluid. In order to characterise possible phase equilibria in confined systems, we should ensure that the grand potential $\Omega_\alpha^{\rm ex}$ for phase α is equal to $\Omega_\beta^{\rm ex}$ for phase β. As $\Omega^{\rm ex}=\gamma A$, this condition can be rephrased as $\gamma_\alpha=\gamma_\beta$. From Eq. 4, we observe that $\Omega^{\rm ex}$ is a function of μ,T,A and L. One possible scenario for investigating phase transitions in a pore is to increase the chemical potential at

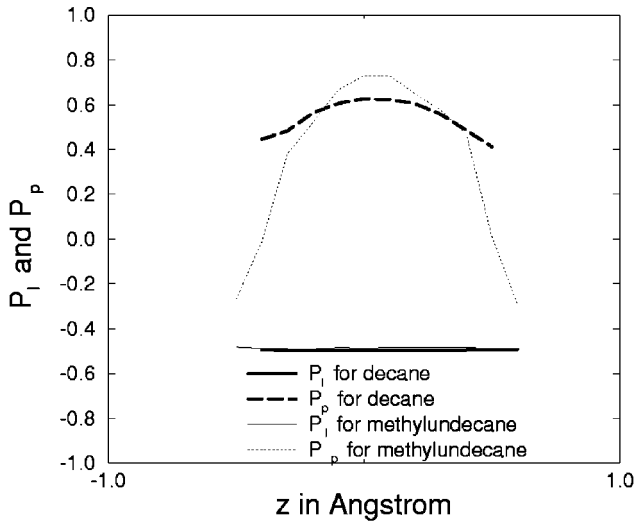

FIG. 11. The order parameters $P_l(z)$ and $P_p(z)$ for a plate separation of 5 Å for *n*-decane and 2-methylundecane.

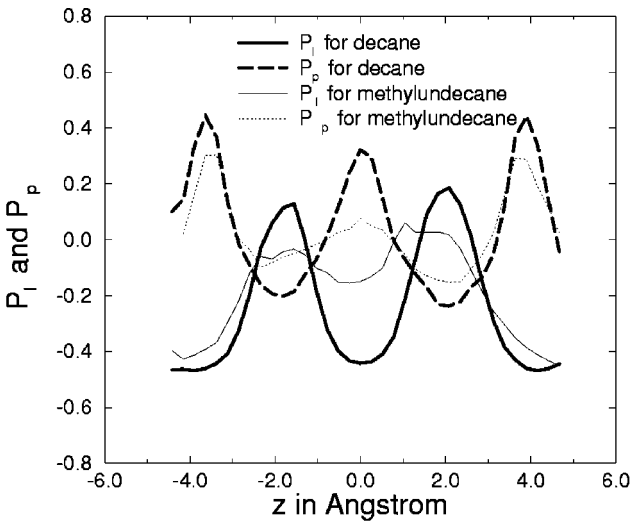

FIG. 13. The order parameters $P_l(z)$ and $P_p(z)$ for a plate separation of 13 Å for *n*-decane and 2-methylundecane.

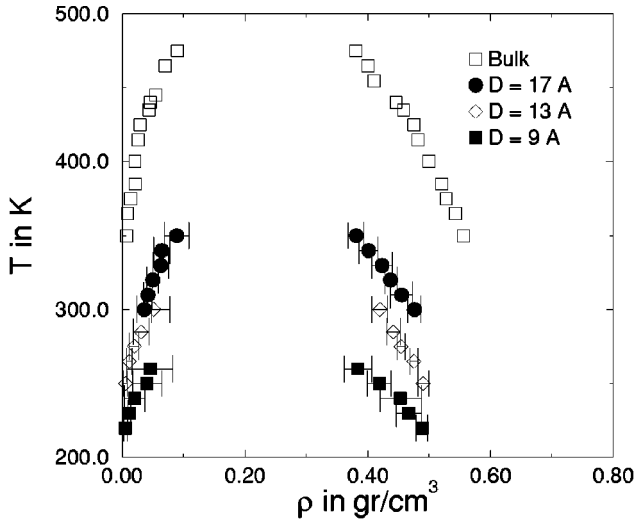

FIG. 14. Liquid-vapour coexistence points obtained from Gibbs ensemble Monte-Carlo simulations for *n*-pentane at a plate separation of 9, 13, and 17 Å. The results for the bulk are taken from Ref. 30.

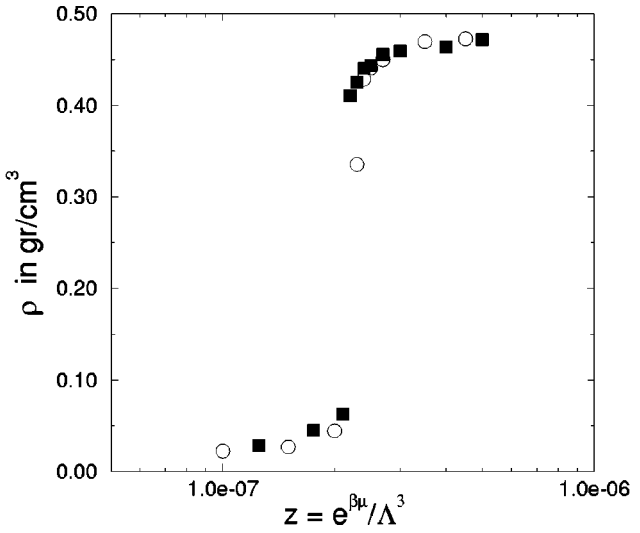

FIG. 15. An adsorption isotherm at a plate separation of 13 Å and at a temperature of 285 K for *n*-pentane versus the fugacity. The open circles are data obtained by increasing the fugacity in subsequent runs, while the solid squares are data obtained by lowering the fugacity. Subsequent runs were started from previously equilibrated configurations.

fixed wall area, temperature, and plate separation. By measuring the adsorption isotherm, i.e., the adsorption in the pore as a function of the chemical potential, one should be able to locate the phase transition. However, due to hysteresis, this procedure is very inaccurate in the determination of the phase coexistence points. Another route to locate phase coexistence is to perform Gibbs ensemble simulations. An extensive derivation of the Gibbs ensemble simulation technique applied for confined systems is given by Panagiotopoulos.[13] However, intuitively, one can understand this as follows. In an ordinary Gibbs ensemble simulation, volume and particles are exchanged between two systems until the volumes and numbers of particles of the separate systems reach stationary values within fluctuations. The resulting systems are those of two coexisting phases at the same pressure due to volume exchange and chemical potential due to particle exchange. In a Gibbs ensemble simulation for confined systems, area and particles are exchanged between the two systems, while the plate separation is kept constant. The exchange of particles ensures equal chemical potential for both phases, while the exchange of area ensures equal fluid-surface interfacial tension in the same spirit as the exchange of volume serves for equal pressure in bulk systems.

We performed Gibbs ensemble simulations for linear pentane for a plate separation of 9, 13, and 17 Å in order to locate the vapour-liquid coexistence region. At a plate separation of 5 Å, we did not find phase coexistence between a liquid and a vapour. The disappearance of the vapour-liquid coexistence has been observed in density functional calculations[35] and computer simulations.[15,16] The results are shown in Fig. 14. The results for the bulk are taken from Ref. 30. We observe that the critical temperature shifts to lower temperatures with decreasing plate separation. This shift of the critical temperature of the liquid-vapour coexistence to lower temperatures upon confining is generic and is explained in Ref. 35. The variable $1/H$ plays a similar role as the temperature. Since Van der Waals, it is known that attraction between the molecules is responsible for the liquid-vapour transition. When the temperature rises the attraction between the molecules becomes less important and above a certain temperature (the critical temperature) the liquid-vapour coexistence disappears. When a fluid is confined between two plates, the attraction is diminished as the number of neighbors decreases. Thus, already at lower temperatures the liquid-vapour region disappears, which results in a lower critical temperature. Similar to the critical temperature, a critical plate separation can be found below which the liquid-vapour transition disappears.

For higher alkanes the critical temperature will also shift to lower temperatures upon confining, as this phenomena is generic. We therefore can conclude that our simulations for measuring the solvation force were sufficiently far from the critical point and the occurrence of any phase transition.

We also performed grand canonical Monte-Carlo simulations for a plate separation of 13 Å, at 285 K, and at different values for the chemical potential. We first increased the chemical potential in subsequent runs and then we lowered the chemical potential. Subsequent runs were started from previously equilibrated configurations. In Fig. 15, we plot the adsorption versus the fugacity $z=\exp(\beta\mu)/\Lambda^3$, where Λ is the de Broglie thermal wavelength. We did not observe any evidence for hysteresis, which was expected from previous simulations.[13,15–17]

VI. CONCLUSIONS

We performed grand canonical Monte-Carlo simulations of a system of *n*-decane, 2-methylheptane and 2-methylundecane between two solid surfaces. We computed the solvation force exerted by the fluid on the plates. We found a large difference in the solvation force for linear and

branched alkanes. For *n*-decane, we found an oscillatory behavior in the solvation force with periodicity close to the width of the molecule. For the branched molecules, we found that the oscillations are decreased and are shifted to the attractive region, which might be the result of interdigitation that links all the molecular layers formed in the fluid. In addition, we computed the liquid-vapour coexisting regions of *n*-pentane confined in a slit of 17, 13, 9 Å. The critical temperature of the liquid-vapour coexistence shifts to lower temperatures upon confining and we can therefore conclude that our simulations for measuring the solvation force, were sufficiently far from the critical point. For a plate separation of 5 Å, we did not find a liquid-vapour transition.

ACKNOWLEDGMENTS

We thank Berend Smit, Sami Karaborni, and A. Levent Demirel for useful discussions, and René van Roij for a critical reading of the manuscript.

[1] R. Evans, J. Phys. Condensed Mater. **2**, 8989 (1990).
[2] J. van der Waals, Ph.D. thesis, The Netherlands, Hoogeschool te Leiden, 1873.
[3] E. Verwey and J. Overbeek, in *Theory of Stability of Lyophobic Colloid* (Elsevier, Amsterdam, 1948).
[4] J. Israelachvili, in *Intermolecular and Surface Forces*, 2nd ed. (Academic, New York, 1992).
[5] J. Israelachvili, Acc. Chem. Res. **20**, 415 (1987).
[6] J. Lane and T. Spurling, Aust. J. Chem. **34**, 1529 (1981).
[7] I. Snook and W. van Megen, J. Chem. Phys. **72**, 2907 (1980).
[8] W. van Megen and I. Snook, J. Chem. Phys. **74**, 1409 (1981).
[9] J. Magda, M. Tirell, and H. Davis, J. Chem. Phys. **83**, 1888 (1985).
[10] D. Henderson and M. Lozada-Cassou, J. Colloid Interface Sci. **114**, 180 (1986).
[11] M. Schoen, D. Diestler, and J. Cushman, J. Chem. Phys. **87**, 5464 (1987).
[12] M. Schoen, J. Cushman, D. Diestler, and J. C. L. Rhykerd, J. Chem. Phys. **88**, 1394 (1988).
[13] A. Panagiotopoulos, Mol. Phys. **62**, 701 (1987).
[14] P. Tarazona, U. Marini Bettolo Marconi, and R. Evans, Mol. Phys. **60**, 573 (1987).
[15] B. Peterson and K. Gubbins, Mol. Phys. **62**, 215 (1987).
[16] B. Peterson *et al.*, J. Chem. Phys. **88**, 6487 (1988).
[17] J. Walton and N. Quirke, Mol. Simul. **2**, 361 (1989).
[18] T. Vanderlick, L. Scriven, and H. Davis, J. Chem. Phys. **90**, 2422 (1989).
[19] D. Courtemanche, T. Pasmore, and F. van Swol, Mol. Phys. **80**, 861 (1993).
[20] J. Israelachvili, S. Kott, M. Gee, and T. Witten, Macromolecules **22**, 4247 (1989).
[21] H. Christenson, D. Gruen, R. Horn, and J. Israelachvili, J. Chem. Phys. **87**, 1834 (1987).
[22] R. Horn and J. Israelachvili, Macromolecules **22**, 4253 (1988).
[23] J. Israelachvili and S. Kott, J. Chem. Phys. **88**, 7162 (1988).
[24] Y. Wang, K. Hill, and J. Harris, J. Chem. Phys. **100**, 3276 (1994).
[25] S. Granick, A. Demirel, L. Cai, and J. Peanasky, Isr. J. Chem. **35**, 75 (1995).
[26] M. Dijkstra, Europhys. Lett. **37**, 281 (1997).
[27] R. Evans and U. M. B. Marconi, J. Chem. Phys. **86**, 7138 (1987).
[28] J. Henderson, Mol. Phys. **59**, 89 (1986).
[29] D. Frenkel and B. Smit, in *Understanding Molecular Simulations: From Algorithms to Applications* (Academic, Boston, 1996)
[30] B. Smit, S. Karaborni, and J. Siepmann, J. Chem. Phys. **102**, 2126 (1995).
[31] W. Steele, Surf. Sci. **36**, 317 (1973).
[32] P. Padilla and S. Toxvaerd, J. Chem. Phys. **101**, 1490 (1994).
[33] D. Frankel, G. Mooij, and B. Smit, J. Phys. Condensed Matter **4**, 3053 (1992).
[34] S. Balasubramanian, M. Klein, and J. Siepmann, J. Phys. Chem. **100**, 11 960 (1996).
[35] R. Evans, U. M. B. Marconi, and P. Tarazona, J. Chem. Phys. **84**, 2376 (1986).